Activin Receptor-Like Kinase 7 Suppresses Lipolysis to Accumulate Fat in Obesity Through Downregulation of Peroxisome Proliferator–Activated Receptor γ and C/EBPα

Satomi Yogosawa,[1] Shin Mizutani,[1] Yoshihiro Ogawa,[2] and Tetsuro Izumi[1]

We previously identified a quantitative trait locus for adiposity, non-insulin-dependent diabetes 5 (*Nidd5*), on mouse chromosome 2. In the current study, we identified the actual genetic alteration at *Nidd5* as a nonsense mutation of the *Acvr1c* gene encoding activin receptor-like kinase 7 (ALK7), one of the type I transforming growth factor-β receptors, which results in a COOH-terminal deletion of the kinase domain. We further showed that the ALK7 dysfunction causes increased lipolysis in adipocytes and leads to decreased fat accumulation. Conversely, ALK7 activation inhibits lipolysis by suppressing the expression of adipose lipases. ALK7 and activated Smads repress those lipases by downregulating peroxisome proliferator–activated receptor γ (PPARγ) and CCAAT/enhancer binding protein (C/EBP) α. Although PPARγ and C/EBPα act as adipogenic transcription factors during adipocyte differentiation, they are lipolytic in sum in differentiated adipocytes and are downregulated by ALK7 in obesity to accumulate fat. Under the obese state, ALK7 deficiency improves glucose tolerance and insulin sensitivity by preferentially increasing fat combustion in mice. These findings have uncovered a net lipolytic function of PPARγ and C/EBPα in differentiated adipocytes and point to the ALK7-signaling pathway that is activated in obesity as a potential target of medical intervention.
***Diabetes* 62:115–123, 2013**

Recent genome-wide association studies in human populations have identified multiple genes associated with common polygenic diseases, including type 2 diabetes and obesity (1). However, because of their intrinsic technical limitations, these studies can only identify common variants of a relatively small effect size and not rare variants of a large effect size. In contrast to human studies, genetic crosses in animal polygenic disease models allow mapping of quantitative trait loci (QTLs), and further, the construction of congenic strains harboring the specific chromosomal segment can easily relate linkage disequilibrium-based association to the physical definition of the responsible gene. The identification of genetic alterations with major effects in animal polygenic diseases will deepen our understanding of human pathophysiology, as has the discovery of causal genes in animal monogenic diseases (2–4). However, such studies are time- and labor-intensive, and few have demonstrated actual gene alterations.

We previously identified non-insulin-dependent diabetes 5 (*Nidd5*) on mouse chromosome 2 that affects adiposity by genetic crosses between Tsumura, Suzuki, Obese Diabetes (TSOD) mice and control BALB/cA (BALB) mice (5). We then generated congenic strains for this QTL and characterized their phenotypes to physically determine its location (6). In the current study, we demonstrate that a nonsense mutation of the *Acvr1c* gene encoding activin receptor-like kinase 7 (ALK7) decreases adiposity. ALK7 deficiency upregulates peroxisome proliferator–activated receptor γ (PPARγ) and CCAAT/enhancer binding protein (C/EBP) α and promotes lipolysis by increasing the expression of adipose lipases, which leads to a net decrease in fat accumulation. Surprisingly, PPARγ and C/EBPα reduce triglyceride (TG) content in sum in mature adipocytes, although they promote both TG synthesis and breakdown. Furthermore, ALK7 deficiency in the obese state ameliorates obesity-induced glucose intolerance and insulin resistance in vivo. These findings suggest that PPARγ and C/EBPα play lipid-mobilizing roles in mature adipocytes and point to the ALK7-signaling pathway as a possible target of therapy for obesity.

RESEARCH DESIGN AND METHODS

Animal procedures. All animal experiments were performed in accordance with the rules and regulations of the Animal Care and Experimentation Committee, Gunma University. Mice had ad libitum access to water and standard laboratory chow (CE-2; CLEA Japan) in an air-conditioned room with 12-h light/dark cycles. The composition of the high-fat diet (HFD) was 55% fat, 28% carbohydrate, and 17% protein (calorie percentage; Oriental Yeast). The TSOD mouse was originally established as an inbred strain with obesity and urinary glucose (7). BALB and C57BL/6N mice were purchased from CLEA Japan. The development of congenic mouse strains for *Nidd5* has been described elsewhere (6). Genotyping was performed using primers listed in Supplementary Table 1. Only male mice were phenotypically characterized in this study. Blood samples were collected from the tail vein. Serum levels of nonesterified fatty acid (NEFA) and glycerol were measured by NEFA C-test (Wako) and Free Glycerol Assay Kit (BioVision), respectively. Oxygen consumption and CO_2 production were measured using the Oxymax system (Columbus Instruments).

Adipocyte isolation. Epididymal fat was excised, minced, and digested with 1 mg/mL collagenase type I (Invitrogen) for 30 min at 37°C under shaking. The cells were filtered through a 250-μm nylon mesh and centrifuged at 50 × *g* for 10 min. The floating adipocytes were washed with PBS twice. The pellet containing the stroma-vascular fraction (SVF) was filtered through a 40-μm nylon mesh and incubated with erythrocyte-lysing buffer (155 mmol/L NH_4Cl, 5.7 mmol/L K_2HPO_4, and 0.1 mmol/L EDTA) at room temperature for 5 min and washed with PBS twice. For immunoblotting and immunoprecipitation, cells were lysed with buffer (20 mmol/L HEPES (pH 7.4), 150 mmol/L NaCl, 1% Triton X-100, 0.2 mmol/L EDTA, and 1 mmol/L dithiothreitol) containing

From the [1]Laboratory of Molecular Endocrinology and Metabolism, Department of Molecular Medicine, Institute for Molecular and Cellular Regulation, Gunma University, Maebashi, Japan; and the [2]Department of Molecular Endocrinology and Metabolism, Graduate School of Medical and Dental Sciences, Tokyo Medical and Dental University, Tokyo, Japan.
Corresponding author: Tetsuro Izumi, tizumi@showa.gunma-u.ac.jp.
Received 9 March 2012 and accepted 30 June 2012.
DOI: 10.2337/db12-0295
This article contains Supplementary Data online at http://diabetes.diabetesjournals.org/lookup/suppl/doi:10.2337/db12-0295/-/DC1.

protease and phosphatase inhibitors. For the lipid metabolic assays, an equal number of freshly isolated adipocytes was used from each mouse strain.

Cell culture. A 3T3-L1 cell line stably expressing coxsackie-adenovirus receptor (CAR) to facilitate adenovirus uptake (8) was cultured in 10% calf serum-containing Dulbecco's modified Eagle's medium. To induce differentiation into mature adipocytes, confluent cells (day 0) were switched to the medium containing 10% FBS, supplemented with 5 μg/mL insulin, 0.5 mmol/L 3-isobutyl-1-metylxanthine, and 0.25 μmol/L dexamethasone for 2 days and subsequently with 5 μg/mL insulin for 2 days.

Quantitative PCR analyses. Total RNA was reverse-transcribed using oligo-$(dT)_{12–18}$ primer and Superscript III (Invitrogen). PCR was then performed with SYBR premix Ex Taq (Takara Bio). The results were normalized against the ribosomal protein 36B4 mRNA expression. The primer sequences are listed in Supplementary Table 2.

Vector construction. Full-length cDNAs for ALK7, Smads, PPARγ2, and C/EBPα were reverse transcribed from RNA of mouse epididymal or 3T3-L1 adipocytes and subcloned in the pcDNA3 vector (Invitrogen) modified to contain a COOH-terminal hemagglutinin tag or COOH-terminal three tandem FLAG tags. All of the mutants were generated using a PCR-based mutagenesis strategy. The short-hairpin RNAs (shRNAs) were designed according to the BLOCK-iT Adenoviral RNAi Expression System (Invitrogen). The primer sequences are listed in Supplementary Table 3.

Lipid assays. Incorporation of [^{14}C]palmitate into TG was measured as described previously (9). Briefly, isolated adipocytes were incubated at 37°C for 2 h in Krebs-Ringer-HEPES buffer containing 1% fatty acid (FA)-free BSA and 0.2 μCi/mL [1-^{14}C]palmitic acid (PerkinElmer). Lipolysis was assessed by measuring the concentration of glycerol. Adipocytes were incubated at 37°C for 3 h in Krebs-Ringer-HEPES buffer containing 2 mmol/L glucose and 1% FA-free BSA with or without 10 μmol/L isoproterenol (Sigma-Aldrich). The TG concentration of cell lysates was measured using a TG Quantification Kit (BioVision) and normalized for protein concentration. Hepatic TG content was measured as described previously (10).

Luciferase reporter assay. CAR–3T3-L1 adipocytes (day 6) were transfected with reporter plasmid containing the indicated gene promoter and control plasmid pGL4.74 [hRluc/TK] (Promega). At 5 h posttransfection, the cells were infected with adenovirus and incubated for a further 43 h. The luciferase activities were measured by the Dual-Luciferase Reporter Assay System (Promega). The primer sequences are listed in Supplementary Table 4.

Chromatin immunoprecipitation assay. This was performed using a ChIP Assay Kit (Millipore). The precipitated and input DNAs were assayed for quantitative PCR using the primers listed in Supplementary Table 5.

Insulin secretion assay. Ten fresh islets isolated as described previously (11) were first incubated at 37°C for 30 min in Krebs-Ringer-HEPES buffer containing 0.1% BSA and 2.8 mmol/L glucose and then for another 30 min in the same buffer containing 16.7 mmol/L glucose. Insulin secreted in each buffer or remained in the cells was measured using an AlphaLISA insulin kit with an EnVision 2101 multilabel reader (PerkinElmer).

Antibodies. Rabbit polyclonal antibody was generated toward the COOH-terminal region (230–493 amino acids) of ALK7 protein and affinity-purified from whole serum using the antigen protein immobilized on a nitrocellulose strip. Other commercially available antibodies are listed in Supplementary Table 6.

Statistical analyses. Statistical significance was determined using two-tailed Student *t* test or one-way ANOVA with Tukey multiple comparison test.

RESULTS

A nonsense mutation of the *Acvr1c* gene in the genome of the BALB mouse. We previously mapped a QTL for adiposity, *Nidd5*, in a 9.5-megabase (Mb) interval between *D2Mit433* and *D2Mit91* on mouse chromosome 2 by phenotypic analysis of congenic strains that carry a control BALB-derived genomic interval and an obese diabetic TSOD background (6). By genotyping of these congenic strains for single nucleotide polymorphisms (SNPs) around the region, we further narrowed the locus to a 1.0-Mb interval between SNPs *rs29504161* and *rs13476526*, which contains five genes (Fig. 1*A*). Sequencing of all the exons and the exon–intron boundaries of these genes, however, revealed no significant mutations in the genome of TSOD mice. Northern blot analysis showed comparable sizes and levels of the gene transcripts between TSOD and BALB mice (data not shown), except for those of the *Acvr1c* gene encoding ALK7 (Fig. 1*B*). Surprisingly, sequencing analysis of the *Acvr1c* gene revealed a mutation in the genome of control BALB mice, which generates a stop codon at the arginine 322 of ALK7 protein. Therefore, the observed difference in the transcript level between the two strains should be due to its decreased levels in BALB mice via a nonsense-mediated mRNA decay mechanism (12). Consistently, polyclonal antibody generated against the COOH-terminal region of ALK7 protein recognized a protein of the expected size (56 kDa) in the white adipose tissue (WAT) and brown adipose tissue (BAT) extracts of TSOD mice, but not in those of BALB mice or the congenic strain T.B-*Nidd5*/3 (6) harboring this *Acvr1c* gene mutation (Fig. 1*C*). The ALK7 transcript and protein were detected only in mature adipocytes but not in the SVF of WAT from the TSOD mice (Fig. 1*D*). Furthermore, ALK7 protein was expressed only in later stages of adipose differentiation in the 3T3-L1 cell line (Fig. 1*E*), which is consistent with previous findings (13).

Increased lipolysis in ALK7-deficient adipocytes. The apparently normal adipose tissue of T.B-*Nidd5*/3 mice (6) indicates that the responsible gene is not involved in adipogenesis. Further, the smaller adipocyte size without a change in the adipocyte number in T.B-*Nidd5*/3 mice (6) suggests that the gene does not directly regulate adipocyte proliferation or apoptosis. Thus, we investigated the activity of lipid metabolism, which could affect the size of the adipocytes and the degree of fat accumulation. Palmitate uptake and its conversion into TG were significantly increased in ALK7-deficient adipocytes from the T.B-*Nidd5*/3 mice compared with those from the TSOD mice (Fig. 2*A*). The transcript levels of the genes involved in those processes were consistently higher. However, the increased TG synthesis should augment adiposity, contrary to the observed phenotype of ALK7-deficient mice. Because mobilization of fat stores predominantly occurs through the hydrolysis of TG into glycerol and FA, the increased lipolysis could account for the decreased fat accumulation in the T.B-*Nidd5*/3 mice. In fact, glycerol release from ALK7-deficient adipocytes was significantly increased in both the basal and isoproterenol-stimulated states (Fig. 2*B*). Consistently, the protein and transcript levels of adipose TG lipase (ATGL) and hormone-sensitive lipase (HSL), two major lipases in WAT (14), were much higher in ALK7-deficient adipocytes (Fig. 2*C*). These findings indicate that ALK7 deficiency promotes both TG synthesis and breakdown, although the net lipid storage appears to be decreased.

ALK7 suppresses lipase expression through Smads 2, 3, and 4. We next investigated whether activation of ALK7 elicits opposite effects on lipolysis in cultured 3T3-L1 adipocytes. In contrast to wild-type (WT) ALK7, constitutively active (CA) ALK7 generated by replacing the threonine 194 with aspartate (15) decreased both protein and transcript levels of ATGL and HSL (Fig. 3*A* and *B*). Accordingly, glycerol release was reduced significantly in both the basal and isoproterenol-stimulated states (Fig. 3*C*). We then investigated the downstream signaling of ALK7. ALK7 is known to phosphorylate Smad2 and/or Smad3, which then form a complex with Smad4 to enter the nucleus (16,17). In fact, CA ALK7, but not WT ALK7, stimulates phosphorylation of Smad2 and Smad3 (Fig. 3*A*). The inert activity of WT ALK7 suggests that its activating ligand is not present in the culture medium of 3T3-L1 adipocytes. When 3T3-L1 adipocytes were infected with adenoviruses encoding shRNAs against those Smads (Fig. 3*D*), shRNA against Smad4 or combined shRNAs against Smad2 and Smad3 blocked CA ALK7-induced inhibition of ATGL and HSL

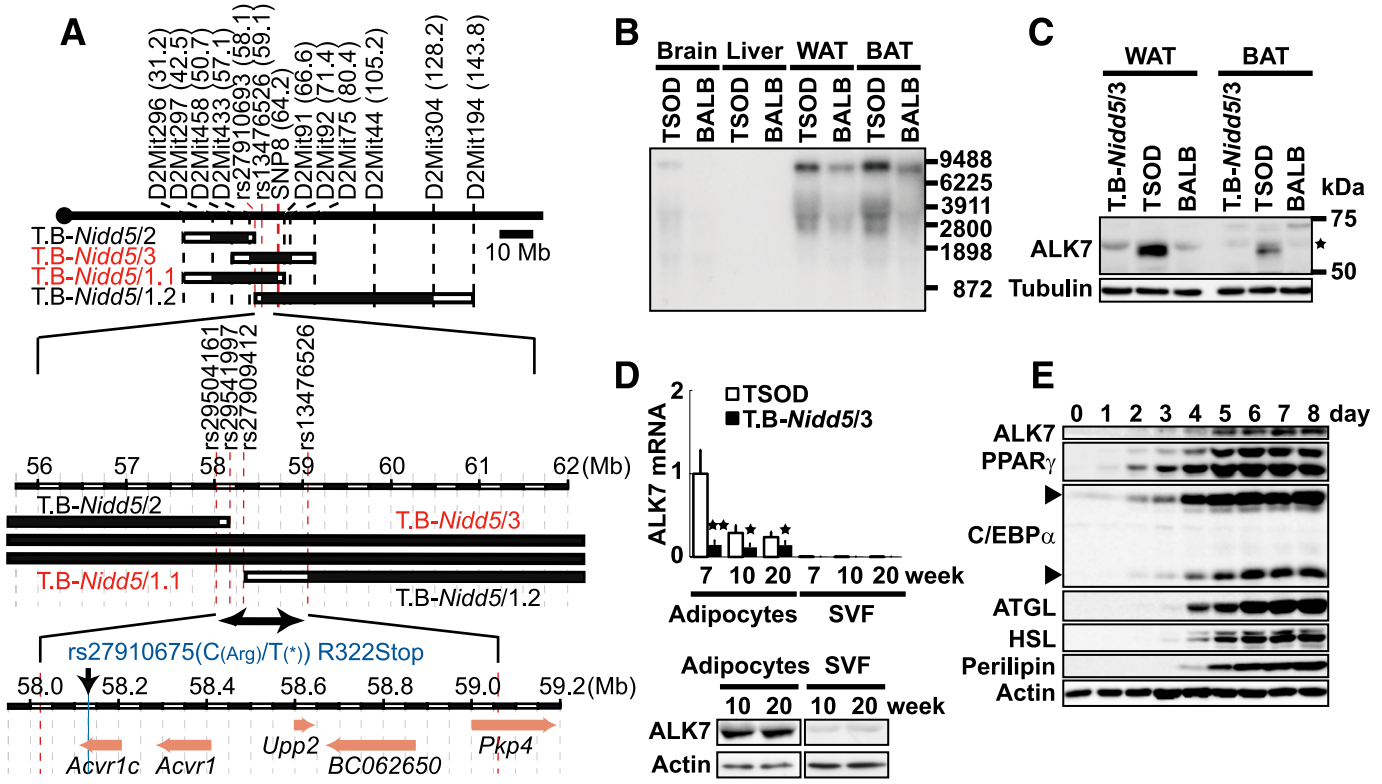

FIG. 1. The *Acvr1c* gene mutation is responsible for the adiposity QTL, *Nidd5*. *A*: Refinement of the *Nidd5* QTL location with four interval-specific congenic strains. Physical positions (Mb) of simple sequence-length polymorphism markers and SNPs are indicated in parentheses. In each strain, a region replaced by a donor BALB genomic interval in a recipient TSOD background is shown by a closed box, whereas flanking intervals in which a crossover occurs are indicated by open boxes. A double-headed arrow indicates a minimal region of *Nidd5* (from *rs29504161* to *rs13476526*) defined by the presence (T.B-*Nidd5*/3 and T.B-*Nidd5*/1.1; red) or absence (T.B-*Nidd5*/2 and T.B-*Nidd5*/1.2; black) of the decreased adipose index of each congenic strain compared with the parental TSOD mouse (6). The BALB genome harbors a functional polymorphism in the exon 6 of the *Acvr1c* gene, *rs27910675* $C_{(Arg)}/T_{(*)}$, which results in a nonsense mutation at the arginine 322 of ALK7 protein. *B*: ALK7 mRNA expression in the brain, liver, WAT, and BAT of TSOD and BALB mice. *C*: ALK7 and α-tubulin protein expression in WAT and BAT (30 μg) isolated from 10-week-old T.B-*Nidd5*/3, TSOD, and BALB mice. *The band shown by an asterisk is a nonspecific protein. *D*: ALK7 mRNA (top) and protein (bottom) expression in adipocytes and SVF from epididymal adipose tissues of 7-, 10-, and 20-week-old TSOD and T.B-*Nidd5*/3 mice. *$P < 0.05$, **$P < 0.01$ vs. TSOD mice. *E*: Protein extracts of CAR–3T3-L1cells differentiated for the indicated time periods were electrophoresed for immunoblotting with antibodies toward the indicated proteins. All quantitative data are means ± SD (n = 3/group).

expression (Fig. 3*E*). These findings suggest that ALK7 downregulates lipase expression through the canonical pathway involving a complex of Smad4 with Smad2 and/or Smad3.

ALK7 suppresses lipase expression through the regulatory elements for PPARγ and C/EBPα. To investigate the regulatory mechanism of lipase gene expression by ALK7/Smads, we performed transactivation assays

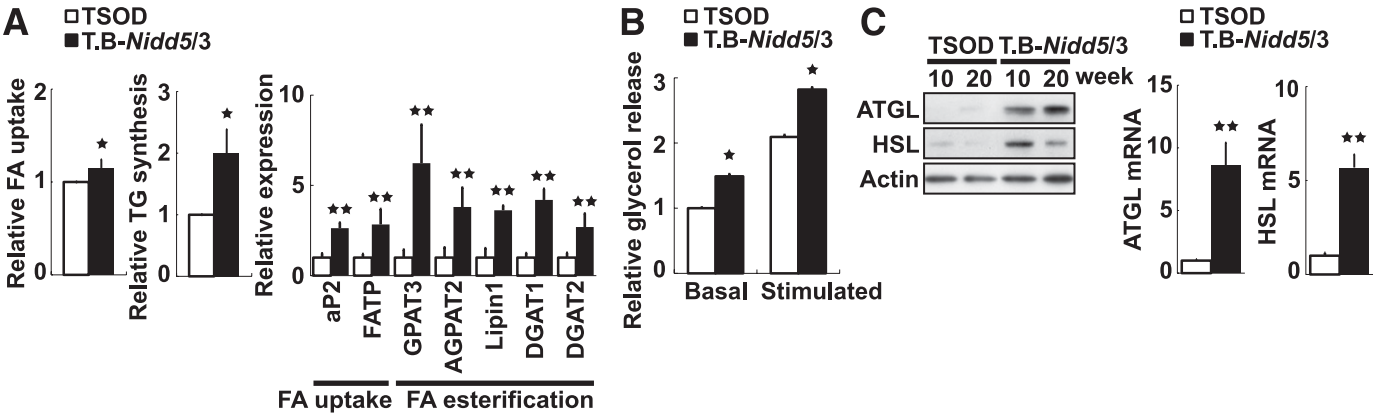

FIG. 2. Loss of functional ALK7 leads to increased lipolysis in mouse adipocytes. *A*: [^{14}C]Palmitate uptake (*left*) and esterification (*middle*) in adipocytes of 11-week-old TSOD (white bars) and T.B-*Nidd5*/3 (black bars) mice. Quantitative PCR analysis of FA uptake- and esterification-related gene expression in the adipocytes of 10-week-old mice (*right*). *B*: Basal and isoproterenol-stimulated glycerol release from adipocytes of 10-week-old mice. *C*: ATGL and HSL protein (*left*) and mRNA (*right*) expression in mouse adipocytes. All quantitative data are means ± SD (n = 3/group). *$P < 0.05$, **$P < 0.01$ vs. TSOD mice.

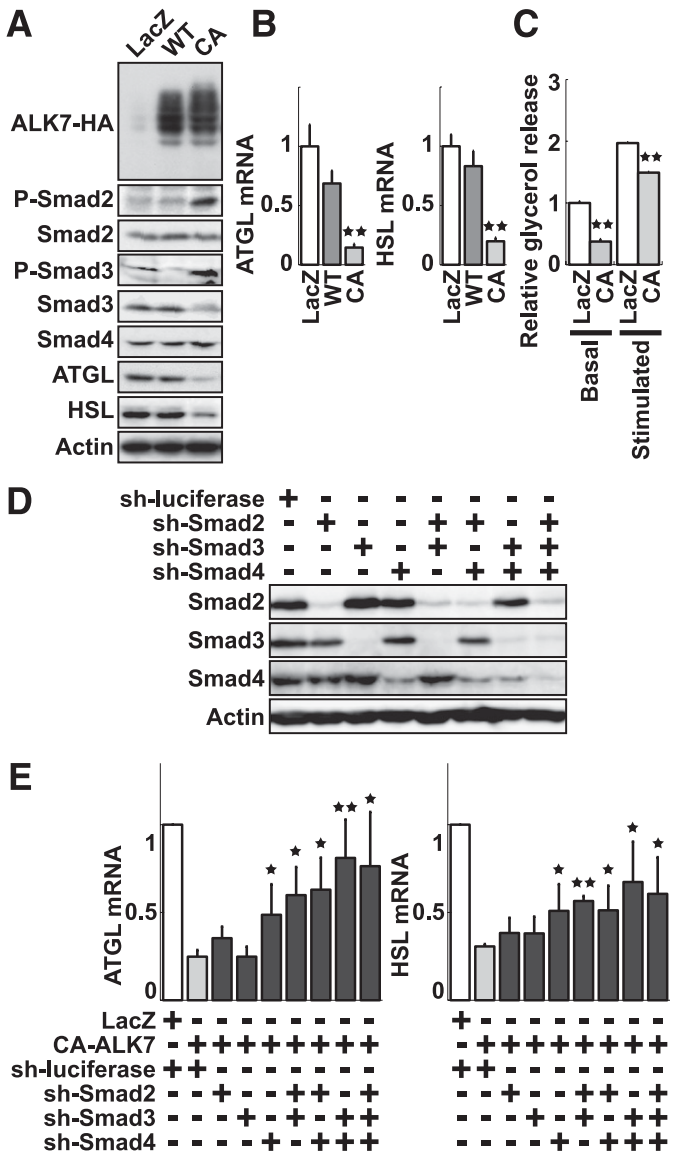

FIG. 3. ALK7 suppresses lipase expression through Smads 2, 3, and 4 in 3T3-L1 adipocytes. Differentiated CAR–3T3-L1 adipocytes were infected with adenovirus encoding LacZ, hemagglutinin-tagged, WT or CA ALK7 on day 5 and were analyzed on day 8 by immunoblotting (*A*), quantitative PCR (*B*), or basal and isoproterenol-stimulated glycerol release assays (*C*). Immunoblotting (*D*) or quantitative PCR analyses (*E*) in CAR–3T3-L1 adipocytes on day 10 after differentiation, which had been infected with adenovirus encoding shRNA against luciferase, Smad2, Smad3, or Smad4 on day 5 and further with that encoding LacZ or CA ALK7 on day 8. All quantitative data are means ± SD (n = 3/group). *$P < 0.05$, **$P < 0.01$ vs. 3T3-L1 cells expressing LacZ (*B* and *C*) or those expressing shRNAs against luciferase and CA ALK7 (*E*).

in 3T3-L1 adipocytes. Because WT ALK7 appears to be inert in those cells (Fig. 3*A* and *B*), we performed the assays with or without the expression of CA ALK7. Smad transcription factors generally bind the consensus sequence, designated as the Smad-binding element (SBE), to regulate gene expression (18). In fact, there are several SBEs in the ATGL and HSL promoter regions. However, the deletion of each of those SBEs had no effect on the repression of the lipases by ALK7 (Fig. 4*A* and *B*), suggesting that ALK7 does not act through the SBEs. Instead, the presence or absence of putative regulatory elements for PPARs and C/EBPs affected the induction of the reporter expressions. In particular, the ATGL promoter activity was markedly reduced in the absence of C/EBP regulatory elements (−3908 to −3896 and −2951 to −2939) or a PPAR regulatory element (−3021 to −3009). In contrast, the HSL promoter activity was markedly reduced by the deletion of three consecutive PPAR regulatory elements (−2061 to −2049, −2048 to −2036, and −1997 to −1985). Chromatin immunoprecipitation (ChIP) assays in 3T3-L1 adipocytes revealed ALK7-sensitive binding of PPARγ and C/EBPα in the −3089 to −2930 region of the ATGL promoter (site 3 in Fig. 4*C*) and of PPARγ in the −2066 to −1965 region of the HSL promoter (site 1 in Fig. 4*D*). By contrast, there was no ALK7-sensitive binding of either C/EBPβ or C/EBPδ, which share a binding sequence with C/EBPα and are known to be involved in adipocyte differentiation (19). These findings indicate that ALK7 represses lipase expression by decreasing the binding of PPARγ and C/EBPα to the lipase promoters.

ALK7 downregulates PPARγ and C/EBPα. We next examined whether ALK7 affects the expression levels of PPARγ and C/EBPα. The protein levels of PPARγ and C/EBPα, but not those of C/EBPβ or C/EBPδ, were markedly upregulated in ALK7-deficient adipocytes (Fig. 5*A*). Consistently, the transcript of adipose-specific PPARγ2 and that of C/EBPα were markedly increased in those cells (Fig. 5*B*). Conversely, when CA ALK7 was expressed in 3T3-L1 adipocytes, PPARγ and C/EBPα were markedly downregulated (Fig. 5*C* and *D*). Furthermore, knockdown of Smad4 or simultaneous knockdown of Smad2 and Smad3 blocked CA ALK7-induced inhibition of PPARγ2 and C/EBPα expression (Fig. 5*E*), as was found in the inhibition of ATGL and HSL expression (Fig. 3*E*). We then investigated the interaction of those Smads with PPARγ and C/EBPα in 3T3-L1 adipocytes (Fig. 5*F*). To make the Smads enter the nucleus efficiently, we constructed CA Smad mutants, in which the COOH-terminal three serine residues are replaced with phosphomimetic aspartate or glutamate residues. When the Smad2 or Smad3 CA mutant or WT Smad4 was singly overexpressed, none of the Smads bound either PPARγ or C/EBPα. However, when Smad4 and CA Smad3 were coexpressed, those complexes interacted with endogenous C/EBPα. Consistent with previous findings from in vitro binding experiments (20), we could find little interaction between Smad2 and C/EBPα, although a much higher expression level of CA Smad2 may be required to detect it. These findings suggest that the Smad complex containing Smad3 titrates C/EBPα to inhibit its transcriptional activity and subsequently to downregulate PPARγ and C/EBPα itself by disrupting a positive-feedback loop for the expression between the two transcription factors (19). Consistent with this idea, the coexpression of Smad4 and CA Smad3 decreased the binding of C/EBPα at site 3 of the ATGL promoter (Fig. 5*G*), which is important for ATGL expression (Fig. 4*A* and *C*). Furthermore, it repressed the transcriptional activation of the ATGL promoter induced by C/EBPα (Fig. 5*H*).

PPARγ and C/EBPα promote lipolysis and decrease TG content in mature adipocytes. Our hypothesis that PPARγ and C/EBPα induce net lipolysis in mature adipocytes is somewhat counterintuitive because those transcription factors are essential for adipogenesis and thus are generally considered to be lipogenic. In fact, the upregulation of those factors in ALK7-deficient adipocytes led to increased TG synthesis (Fig. 2*A*). We thus investigated the net effect of PPARγ2 and C/EBPα in fully differentiated 3T3-L1 adipocytes. The expression of either PPARγ2 or C/EBPα at levels >5–10-fold above the endogenous levels increased the expression of both ATGL and HSL, promoted

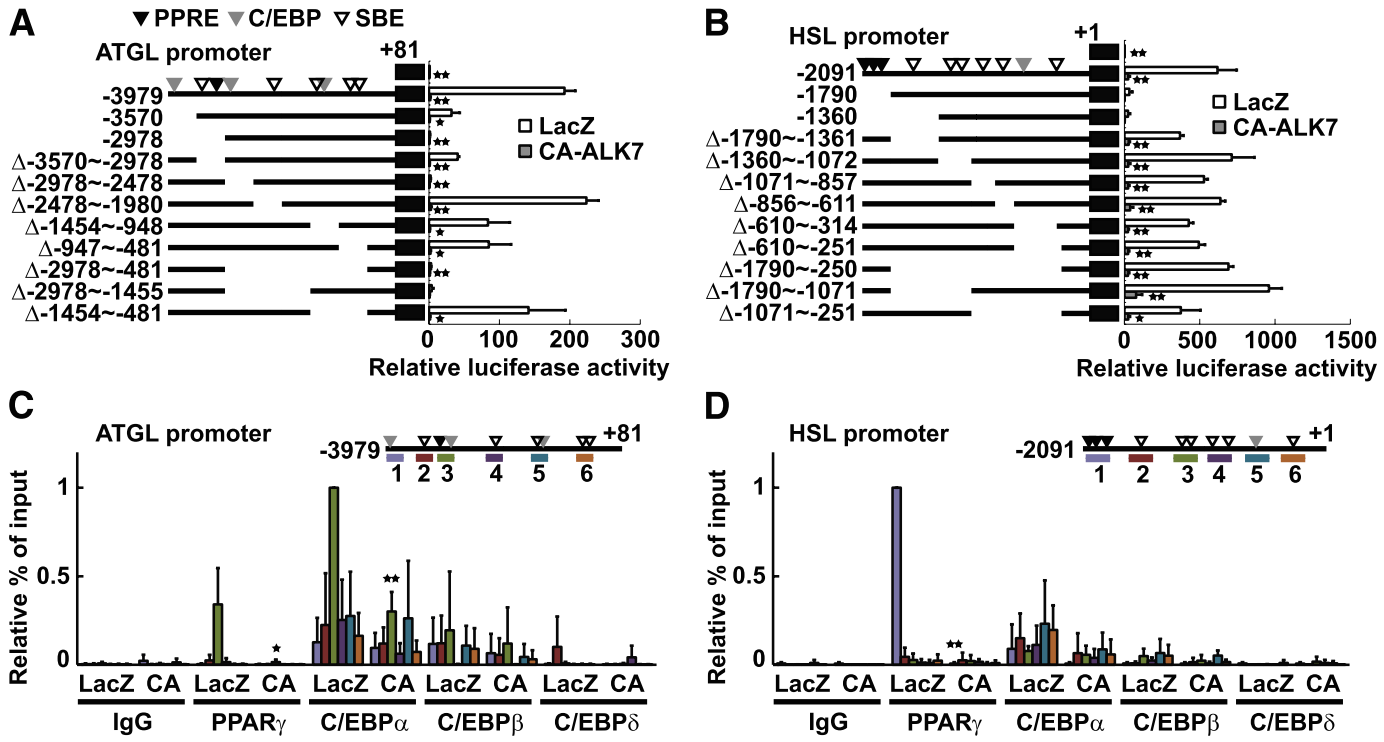

FIG. 4. ALK7 suppresses transcription of ATGL and HSL not through the SBEs but through the regulatory elements for PPAR and C/EBP. Luciferase assays for ATGL (*A*) or HSL (*B*) promoter constructs transfected into CAR–3T3-L1 adipocytes expressing LacZ or CA ALK7. ChIP assays of PPARγ, C/EBPα, C/EBPβ, and C/EBPδ on the ATGL (*C*) or HSL (*D*) promoter in CAR–3T3-L1 adipocytes expressing LacZ or CA ALK7. All data are means ± SD (*n* = 3/group). **P* < 0.05, ***P* < 0.01 vs. 3T3-L1 cells expressing LacZ.

lipolysis, and decreased the TG content (Fig. 6*A*). PPARγ2 had more potent effects on lipolysis than did C/EBPα, despite the weaker effects on the expression of ATGL and HSL, which suggests that PPARγ2 might influence the expression of lipolysis-promoting factors other than those lipases. We also examined the effects of the PPARγ agonist, thiazolidinedione (TZD). Troglitazone treatment of 3T3-L1 adipocytes caused similar effects found in the cells overexpressing PPARγ2: the increased expression of ATGL and HSL as well as an established PPARγ target gene aP2, the promotion of lipolysis, and the decrease of TG content (Fig. 6*B*). Furthermore, troglitazone administration in TSOD mice increased serum levels of NEFAs and glycerol, indicating that PPARγ activation increases lipolysis in vivo (Fig. 6*C*). Interestingly, troglitazone increased the expression of ALK7 itself as well as lipolytic and lipogenic genes, suggesting that ALK7 may be a PPARγ target. Conversely, knockdown of PPARγ or C/EBPα by specific shRNAs induced opposite effects in 3T3-L1 adipocytes: it reduced lipase expression, decreased lipolysis, and increased TG content (Fig. 6*D*). It should be noted that the downregulation of PPARγ decreased the expression of C/EBPα and vice versa (Fig. 6*D*), because the expression and activity of the two factors are mutually dependent (19). Nevertheless, these findings indicate that both PPARγ and C/EBPα induce net lipolysis and decrease fat mass in sum in mature adipocytes.

Improved metabolic indices in obese ALK7-deficient mice. Elevated lipolysis can result in an excess supply of NEFAs to the circulating blood and organs and may cause lipid accumulation and insulin resistance in peripheral tissues. However, the ALK7-deficient T.B-*Nidd5*/3 mice with lower body weight showed enhanced glucose tolerance and insulin sensitivity compared with the TSOD mice (Fig. 7*A*). It has been reported that, although pancreatic islets from lean ALK7-deficient mice exhibit normal insulin secretion in response to initial glucose stimulation, they show enhanced insulin secretion under sustained glucose stimulation (21). We, however, found that islets from T.B-*Nidd5*/3 mice reveal no significant change in glucose-induced insulin secretion and that the expression level of ALK7 in islets is much lower than that in WAT (Fig. 7*B*). Measurement of metabolic rates revealed increased O_2 consumption, decreased respiratory quotients, and increased energy expenditure in T.B-*Nidd5*/3 mice (Fig. 7*C*). Furthermore, in contrast to lean ALK7-deficient mice (21), T.B-*Nidd5*/3 mice exhibited decreased hepatic TG content compared with TSOD mice (Fig. 7*D*). Contrary to expectation from the increased lipolysis in adipocytes, serum levels of NEFAs and glycerol were decreased in T.B-*Nidd5*/3 mice compared with TSOD mice (Fig. 7*E*). The decreased serum levels likely reflect the already decreased fat mass due to net lipolysis continuing from the birth of ALK7-deficient mice. Furthermore, elevated lipolysis subsequently increases FA oxidation at the whole body level, and NEFAs released from adipocytes can be efficiently cleared from the serum. We finally examined the effects of obesity and HFD on the expression levels of ALK7 and growth/differentiation factor 3 (GDF3), which has recently been suggested as a natural ligand of ALK7 because of the coexpression in adipose tissue, the capability of exogenous ALK7 expression to mediate GDF3-dependent signaling in heterologous cells, and the similarity in phenotypes between GDF3- and ALK7-deficient mice (22). The expression level of ALK7 was decreased modestly in C57BL/6 mice under an HFD and in obese TSOD mice compared with C57BL/6 mice under normal chow (Fig. 7*F*). By contrast,

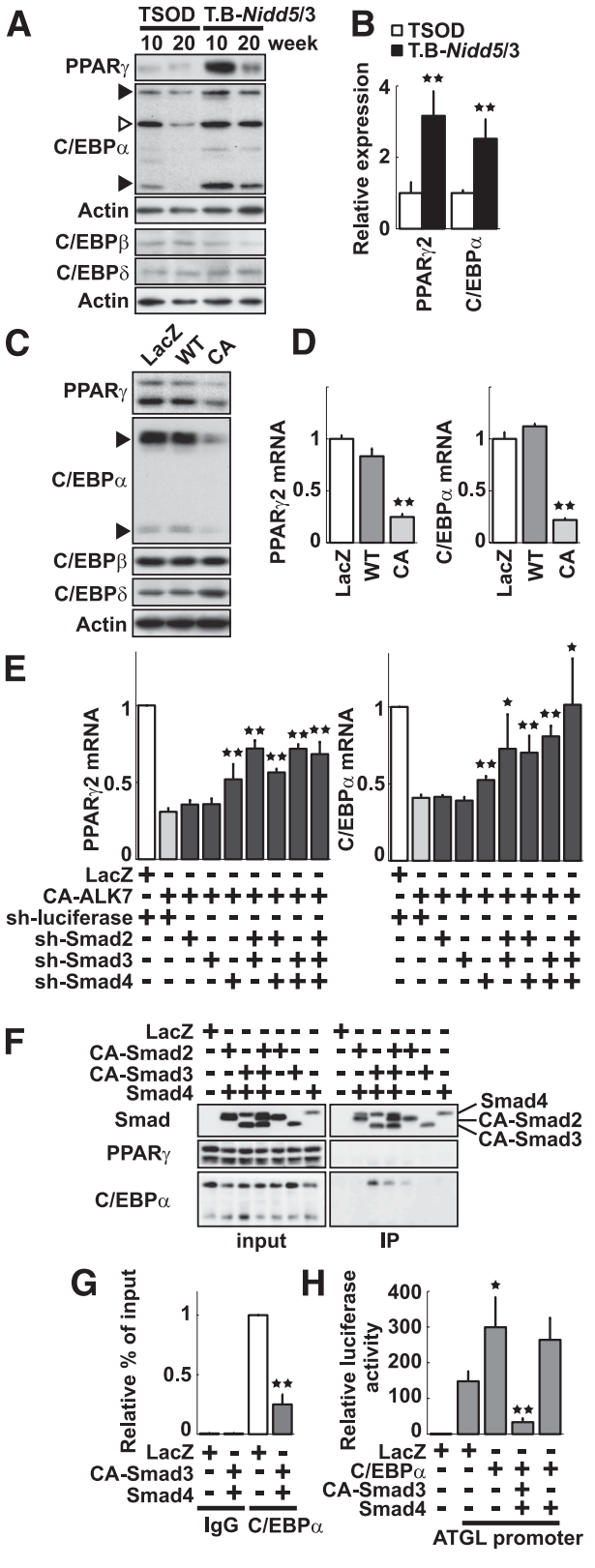

FIG. 5. ALK7 downregulates PPARγ and C/EBPα. *A*: PPARγ, C/EBPα, C/EBPβ, C/EBPδ, and β-actin protein expression in adipocytes from 10- and 20-week-old TSOD and T.B-*Nidd5*/3 mice. Closed arrowheads indicate the positions of full-length (p42) and alternatively translated (p30) C/EBPα proteins (41). The protein indicated by an open arrowhead appears to be a degradation product, which is seen only in the extracts of mouse adipocytes (*A*), but not in those of 3T3-L1 adipocytes (*C*). *B*: PPARγ2 and C/EBPα mRNA expression in mouse adipocytes isolated from 10-week-old TSOD and T.B-*Nidd5*/3 mice. *C*: PPARγ, C/EBPα, C/EBPβ, C/EBPδ, and β-actin protein expression in CAR–3T3-L1 adipocytes that were infected with adenovirus encoding LacZ, WT, or CA ALK7. *D*: PPARγ2 and C/EBPα mRNA expression in CAR–3T3-L1 adipocytes expressing LacZ, WT, or CA ALK7. *E*: Quantitative PCR analyses of PPARγ2 and C/EBPα mRNA expression in CAR–3T3-L1 adipocytes infected with adenoviruses expressing shRNAs against Smads and CA ALK7 as described in Fig. 3*E*. *F*: Complex formation of PPARγ or C/EBPα with Smads in CAR–3T3-L1 adipocytes (day 8) expressing FLAG-tagged, CA Smad2, CA Smad3, and/or WT Smad4. *G*: ChIP assays of C/EBPα on the site 3 region of the ATGL promoter (Fig. 4*C*) in CAR–3T3-L1 adipocytes expressing LacZ or those expressing CA Smad3 and WT Smad4. *H*: Luciferase assays for ATGL promoter in CAR–3T3-L1 adipocytes expressing LacZ, C/EBPα, CA Smad3, and/or WT Smad4. All quantitative data are means ± SD (n = 3/group). *$P < 0.05$, **$P < 0.01$ vs. TSOD mice (*B*), 3T3-L1 cells expressing LacZ (*D*, *G*, and *H*), or shRNAs against luciferase and CA ALK7 (*E*).

the expression of GDF3 was markedly induced under the high-fat dietary condition, as reported previously (23), and in the obese state. These findings suggest that ALK7 can be downregulated secondarily by robust induction of its ligand under nutrient excess.

DISCUSSION

We have successfully identified a mutation of the *Acvr1c* gene at the *Nidd5* QTL, which affects adiposity and body weight in mice. Unexpectedly, the mutation is not derived from the obese TSOD strain but from the control BALB strain. A nonsense mutation of the *Acvr1c* gene in the BALB genome results in a deletion of the kinase domain of encoded ALK7 protein. Thus, BALB mice should be used with caution particularly for metabolic analyses. We demonstrate that loss of ALK7 function leads to elevated lipolysis and decreased fat mass, which explains the phenotypes of the congenic T.B-*Nidd5*/3 strain: lower body weight and a much lower adipose index without any significant changes in food intake, total activity, or adaptive thermogenesis (6). Furthermore, our findings offer the missing mechanism to explain the lean phenotypes of recently characterized ALK7 knockout mice, which exhibit no change in body weight or fat weight under normal chow, but do exhibit reduced weight gain and reduced fat accumulation under HFD (22). ALK7 strongly depresses the expressions of ATGL and HSL through Smads 2, 3, and 4, which appear to act *trans* through binding C/EBPα to inhibit its transactivation function. This interrupts the positive-feedback loop between C/EBPα and PPARγ and markedly decreases the expression of those transcription factors and adipose lipases (Fig. 7*G*).

Consistent with our model, it has been shown that treatment with PPARγ agonists such as TZDs activate adipose tissue lipolysis (24–28). At the whole-body level, it has been shown that troglitazone administration increases the number of small adipocytes in obese rats (29) and that the transgenic mice expressing constitutively activated PPARγ selectively in mature adipocytes have smaller adipocyte size (30). In the current study, we have demonstrated that upregulation of PPARγ or C/EBPα results in elevated lipolysis and decreased TG content both in differentiated adipocytes and in mouse adipose tissue, whereas their downregulation causes the opposite effects. Based on these findings, we propose that PPARγ and C/EBPα play a pivotal role in the lipid remodeling of mature adipocytes and that their dysfunction leads to decreased mobilization of TG and increased fat accumulation in adipocytes. In fact, impaired adipose lipolysis, as well as decreased expression

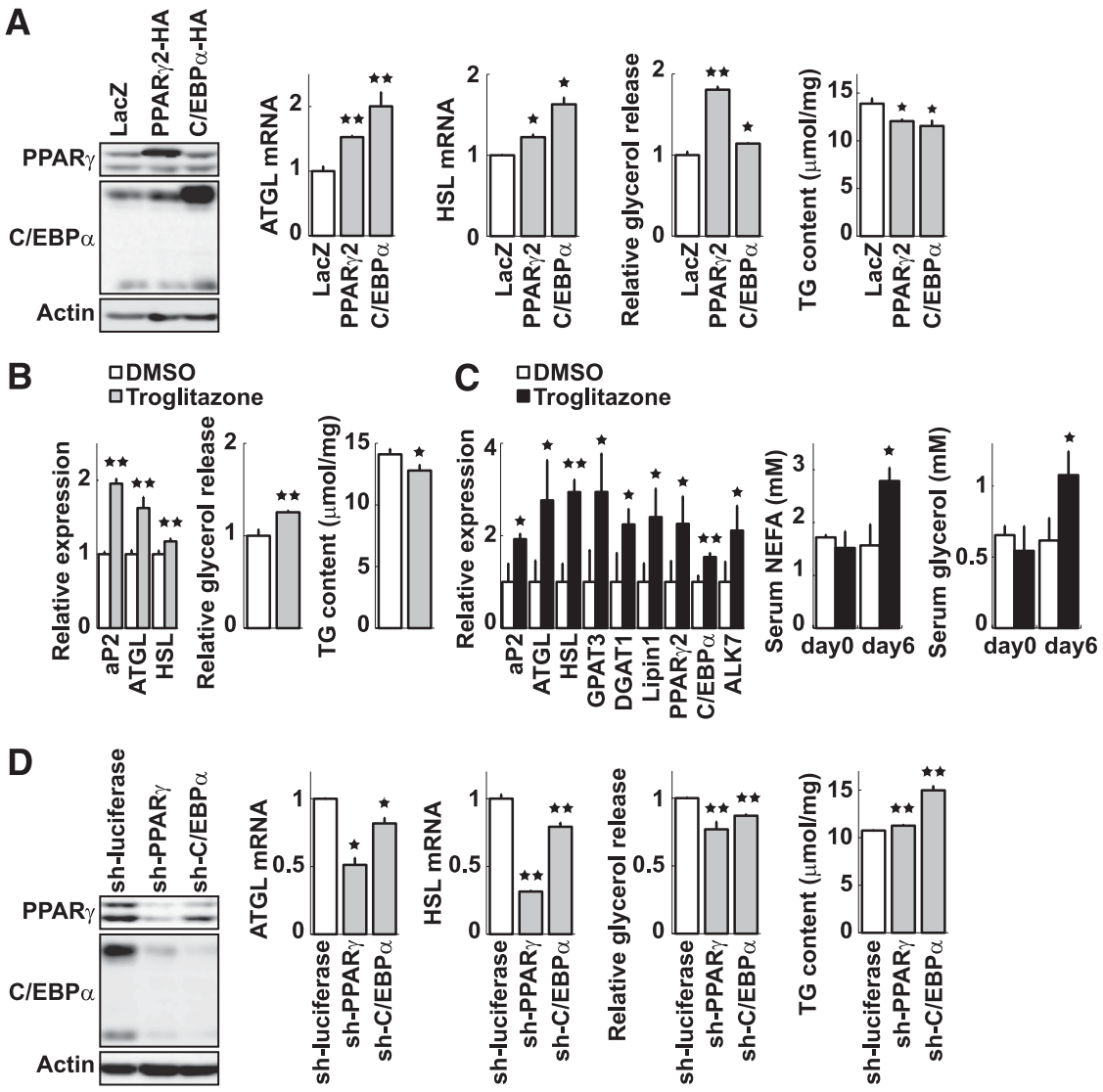

FIG. 6. PPARγ and C/EBPα promote lipolysis and decrease TG content in fully differentiated adipocytes. *A*: Protein expression levels of PPARγ and C/EBPα, mRNA expression levels of ATGL and HSL, glycerol release, and TG content in CAR–3T3-L1 adipocytes (day 9) that had been infected with adenovirus encoding LacZ, PPARγ2, or C/EBPα for 4 days. *B*: Measurement of aP2, ATGL, and HSL mRNA expression levels, glycerol release, and TG content in CAR–3T3-L1 adipocytes (day 10) that had been treated with DMSO or troglitazone (1 μmol/L) for 4 days. *C*: mRNA expression levels in WAT and serum NEFA and glycerol levels in TSOD (17–20-week-old) mice injected intraperitoneally with DMSO or troglitazone (10 mg/kg) for 6 days. *D*: Protein expression levels of PPARγ and C/EBPα, mRNA expression levels of ATGL and HSL, glycerol release, and TG content in CAR–3T3-L1 adipocytes (day 9) that had been infected with adenovirus encoding shRNA against luciferase, PPARγ (common sequence to PPARγ1 and PPARγ2), or C/EBPα for 4 days. All quantitative data are means ± SD (*n* = 3/group). **P* < 0.05, ***P* < 0.01 vs. cells expressing LacZ (*A*) or shRNA against luciferase (*D*), DMSO-treated cells (*B*), or TSOD mice (*C*).

of HSL and ATGL, has been observed in obese human subjects (31–34). Dysfunction of PPARγ and C/EBPα may well be a hallmark of obesity, as was found in the adipocytes of TSOD mice. Although clinical treatment of obesity-associated insulin resistance with TZDs causes significant weight gain, this side effect has recently been shown to be mediated via brain PPARγ, not via adipocyte PPARγ (35,36). Because ALK7 is scarcely expressed in brain (37 and the current study), the inhibition of ALK7 should not produce such weight gain, as in the case of T.B-*Nidd5*/3 mice.

ALK7 is not essential for adipocyte differentiation because both ALK7 knockout mice and ALK7-deficient T.B-*Nidd5*/3 mice show apparently normal development of adipose tissues (6,22). Consistently, ALK7 is not expressed in preadipocytes but is expressed in the late phase of adipocyte differentiation. Because ALK7-knockout mice show reduced fat accumulation only in the face of diet-induced obesity (22), it is likely that ALK7 is activated by chronic nutritional excess to accumulate fat in mature adipocytes by inhibiting lipolysis. However, ALK7 transcripts have been shown to be modestly reduced in the adipose tissue of obese individuals (37). Although we also found the modestly decreased level of ALK7 in obese mice, the expression of GDF3, a candidate ligand of ALK7 (22), was significantly induced under the HFD and obese conditions. Therefore, it is possible that ALK7 is actually activated by its ligand induction under nutrient excess to accumulate fat in adipocytes. Future studies should attempt to elucidate the regulatory mechanism for the expression and secretion of GDF3 and other possible ALK7 ligands.

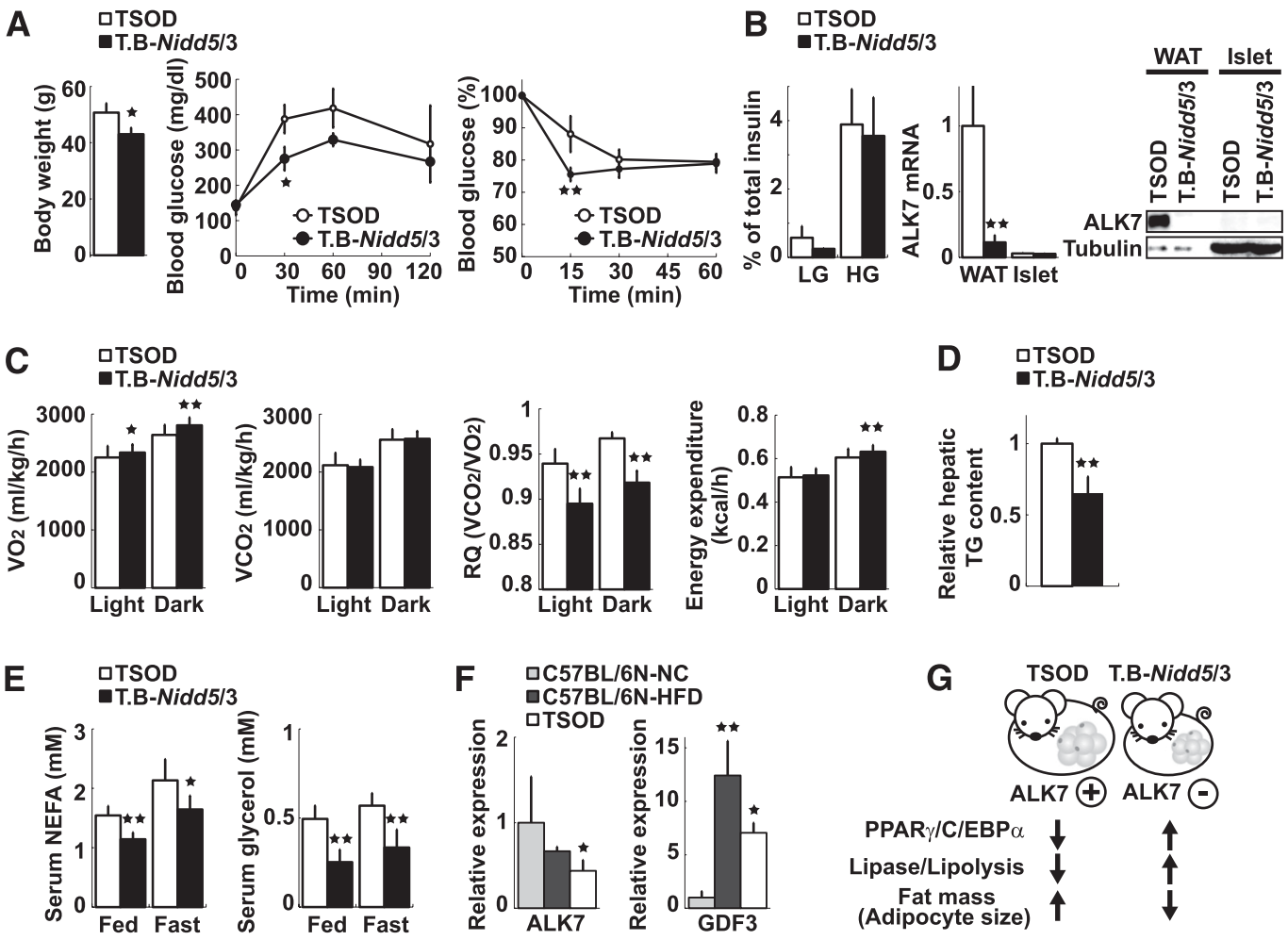

FIG. 7. Loss of functional ALK7 ameliorates metabolic phenotypes of TSOD mice. *A*: Body weight (*left*), blood glucose levels during intraperitoneal glucose tolerance test (1 g/kg body weight) after 12-h fasting (*middle*), and blood glucose levels during intraperitoneal insulin tolerance test (0.75 units/kg body weight; *right*) at the age of 10 weeks. *B*: Insulin secretion from pancreatic islets (*left*), ALK7 mRNA (*middle*) and protein (*right*) expression in WAT and islets from 17–19-week-old TSOD and T.B-*Nidd5/3* mice. Note that 5 μg WAT and 50 μg islet protein extracts was loaded per lane. *C*: Measurement of O_2 consumption, CO_2 production, respiratory quotients (RQ), and energy expenditure during light and dark periods of 10-week-old TSOD and T.B-*Nidd5/3* mice in a metabolic chamber. *D*: Hepatic TG content in 10-week-old TSOD and T.B-*Nidd5/3* mice. *E*: Serum NEFA and glycerol levels in 12-week-old TSOD and T.B-*Nidd5/3* mice that had been fed or fasted for 24 h. *F*: ALK7 and GDF3 mRNA expression in WAT from C57BL/6N mice fed under normal chow (NC) or HFD and TSOD mice. HFD was given to 3-week-old mice for 10 weeks before dissection of epididymal fat. *G*: Comparison of the phenotypes and underlying molecular events between the obese mice with and without ALK7 function. All quantitative data are means ± SD (n = 3–7/group). *$P < 0.05$, **$P < 0.01$ vs. TSOD mice by t test (*A–E*) or vs. C57BL/6N mice fed under NC or by one-way ANOVA (*F*). HG, high glucose; LG, low glucose.

Increased lipolysis from adipocytes can elevate circulating FA levels, induce ectopic fat accumulation, and thus cause insulin resistance. In fact, it has been shown that lean ALK7-deficient mice exhibit hepatic steatosis and insulin resistance as they age (21). In the current study, however, we could not detect any adverse effects of ALK7 deficiency in the presence of obesity. Compared with the parental TSOD mice, the ALK7-deficient T.B-*Nidd5/3* congenic mice show improved glucose tolerance and insulin sensitivity with preferential fat combustion at the whole-body level, probably through increased FA supply from adipocytes. Furthermore, they exhibit no elevation of serum NEFAs or hepatic TG content. Therefore, ALK7 deficiency causes differential effects on insulin sensitivity between obese and lean states, dependent on the amount of TG in adipocytes. These findings are consistent with recent findings in human adipose tissue that lipolysis is an important determinant of lipid removal and that the rate of TG removal from adipocytes has an impact on whole-body insulin sensitivity (38). The decreases in fat accumulation and in adipocyte size in obese ALK7-deficient mice could alleviate chronic inflammation (39) and/or change adipocytokine repertoires (40). In fact, adipocytes from the T.B-*Nidd5/3* mice show lower levels of inflammatory cytokines such as tumor necrosis factor-α and monocyte chemotactic protein-1 than do those from TSOD mice (S.Y. and T.I., unpublished observations). Thus, the inhibition of ALK7 function in adipocytes has a beneficial effect in obesity and provides a rational basis for therapy aimed at the metabolic dysfunction commonly associated with obesity.

ACKNOWLEDGMENTS

This work was supported by grants-in-aid for scientific research and a grant of the Global Centers of Excellence program from Ministry of Education, Culture, Sports, Science and Technology of Japan and in part by grants from the Mitsubishi Foundation and a Novo Nordisk Insulin Study Award (T.I.).

No other potential conflicts of interest relevant to this article were reported.

S.Y. performed functional analyses of ALK7. S.M. performed genetic analyses of mice. Y.O. contributed reagents and helped with data interpretation. T.I. supervised all aspects of study design and interpretation and wrote the manuscript with the assistance of the other authors. T.I. is the guarantor of this work and, as such, had full access to all the data in the study and takes responsibility for the integrity of the data and the accuracy of the data analysis.

The authors thank Drs. Hiroshi Sakaue (Tokushima University) and Ayaka Ito (Tokyo Medical and Dental University) for advice about induction of 3T3-L1 preadipocyte differentiation; Dr. Tadahiro Kitamura (Gunma University) for advice about ChIP assays; Takae Nara, Eri Kobayashi, and Takeshi Ushigome (Gunma University) for colony maintenance of mice; and Junko Toshima (Gunma University) for assistance in preparing the manuscript.

REFERENCES

1. O'Rahilly S. Human genetics illuminates the paths to metabolic disease. Nature 2009;462:307–314
2. Bultman SJ, Michaud EJ, Woychik RP. Molecular characterization of the mouse agouti locus. Cell 1992;71:1195–1204
3. Zhang Y, Proenca R, Maffei M, Barone M, Leopold L, Friedman JM. Positional cloning of the mouse *obese* gene and its human homologue. Nature 1994;372:425–432
4. Wang J, Takeuchi T, Tanaka S, et al. A mutation in the insulin 2 gene induces diabetes with severe pancreatic β-cell dysfunction in the Mody mouse. J Clin Invest 1999;103:27–37
5. Hirayama I, Yi Z, Izumi S, et al. Genetic analysis of obese diabetes in the TSOD mouse. Diabetes 1999;48:1183–1191
6. Mizutani S, Gomi H, Hirayama I, Izumi T. Chromosome 2 locus *Nidd5* has a potent effect on adiposity in the TSOD mouse. Mamm Genome 2006;17:375–384
7. Suzuki W, Iizuka S, Tabuchi M, et al. A new mouse model of spontaneous diabetes derived from ddY strain. Exp Anim 1999;48:181–189
8. Ito A, Suganami T, Miyamoto Y, et al. Role of MAPK phosphatase-1 in the induction of monocyte chemoattractant protein-1 during the course of adipocyte hypertrophy. J Biol Chem 2007;282:25445–25452
9. Listenberger LL, Han X, Lewis SE, et al. Triglyceride accumulation protects against fatty acid-induced lipotoxicity. Proc Natl Acad Sci USA 2003;100:3077–3082
10. Wang XL, Suzuki R, Lee K, et al. Ablation of ARNT/HIF1β in liver alters gluconeogenesis, lipogenic gene expression, and serum ketones. Cell Metab 2009;9:428–439
11. Wang H, Ishizaki R, Kobayashi E, Fujiwara T, Akagawa K, Izumi T. Loss of granuphilin and loss of syntaxin-1A cause differential effects on insulin granule docking and fusion. J Biol Chem 2011;286:32244–32250
12. Amrani N, Sachs MS, Jacobson A. Early nonsense: mRNA decay solves a translational problem. Nat Rev Mol Cell Biol 2006;7:415–425
13. Kogame M, Matsuo S, Nakatani M, et al. ALK7 is a novel marker for adipocyte differentiation. J Med Invest 2006;53:238–245
14. Lafontan M, Langin D. Lipolysis and lipid mobilization in human adipose tissue. Prog Lipid Res 2009;48:275–297
15. Massagué J. TGF-β signal transduction. Annu Rev Biochem 1998;67:753–791
16. Miyazawa K, Shinozaki M, Hara T, Furuya T, Miyazono K. Two major Smad pathways in TGF-β superfamily signalling. Genes Cells 2002;7:1191–1204
17. Schmierer B, Hill CS. TGFβ-SMAD signal transduction: molecular specificity and functional flexibility. Nat Rev Mol Cell Biol 2007;8:970–982
18. Massagué J, Seoane J, Wotton D. Smad transcription factors. Genes Dev 2005;19:2783–2810
19. Farmer SR. Transcriptional control of adipocyte formation. Cell Metab 2006;4:263–273
20. Choy L, Derynck R. Transforming growth factor-β inhibits adipocyte differentiation by Smad3 interacting with CCAAT/enhancer-binding protein (C/EBP) and repressing C/EBP transactivation function. J Biol Chem 2003;278:9609–9619
21. Bertolino P, Holmberg R, Reissmann E, Andersson O, Berggren PO, Ibáñez CF. Activin B receptor ALK7 is a negative regulator of pancreatic beta-cell function. Proc Natl Acad Sci USA 2008;105:7246–7251
22. Andersson O, Korach-Andre M, Reissmann E, Ibáñez CF, Bertolino P. Growth/differentiation factor 3 signals through ALK7 and regulates accumulation of adipose tissue and diet-induced obesity. Proc Natl Acad Sci USA 2008;105:7252–7256
23. Shen JJ, Huang L, Li L, Jorgez C, Matzuk MM, Brown CW. Deficiency of growth differentiation factor 3 protects against diet-induced obesity by selectively acting on white adipose. Mol Endocrinol 2009;23:113–123
24. Kalderon B, Mayorek N, Ben-Yaacov L, Bar-Tana J. Adipose tissue sensitization to insulin induced by troglitazone and MEDICA 16 in obese Zucker rats in vivo. Am J Physiol Endocrinol Metab 2003;284:E795–E803
25. Festuccia WT, Laplante M, Berthiaume M, Gélinas Y, Deshaies Y. PPARγ agonism increases rat adipose tissue lipolysis, expression of glyceride lipases, and the response of lipolysis to hormonal control. Diabetologia 2006;49:2427–2436
26. Kim JY, Tillison K, Lee JH, Rearick DA, Smas CM. The adipose tissue triglyceride lipase ATGL/PNPLA2 is downregulated by insulin and TNF-α in 3T3-L1 adipocytes and is a target for transactivation by PPARgamma. Am J Physiol Endocrinol Metab 2006;291:E115–E127
27. Kershaw EE, Schupp M, Guan HP, Gardner NP, Lazar MA, Flier JS. PPARgamma regulates adipose triglyceride lipase in adipocytes in vitro and in vivo. Am J Physiol Endocrinol Metab 2007;293:E1736–E1745
28. Wang P, Renes J, Bouwman F, Bunschoten A, Mariman E, Keijer J. Absence of an adipogenic effect of rosiglitazone on mature 3T3-L1 adipocytes: increase of lipid catabolism and reduction of adipokine expression. Diabetologia 2007;50:654–665
29. Okuno A, Tamemoto H, Tobe K, et al. Troglitazone increases the number of small adipocytes without the change of white adipose tissue mass in obese Zucker rats. J Clin Invest 1998;101:1354–1361
30. Sugii S, Olson P, Sears DD, et al. PPARγ activation in adipocytes is sufficient for systemic insulin sensitization. Proc Natl Acad Sci USA 2009;106:22504–22509
31. Jensen MD, Haymond MW, Rizza RA, Cryer PE, Miles JM. Influence of body fat distribution on free fatty acid metabolism in obesity. J Clin Invest 1989;83:1168–1173
32. Bougnères P, Stunff CL, Pecqueur C, Pinglier E, Adnot P, Ricquier D. In vivo resistance of lipolysis to epinephrine. A new feature of childhood onset obesity. J Clin Invest 1997;99:2568–2573
33. Langin D, Dicker A, Tavernier G, et al. Adipocyte lipases and defect of lipolysis in human obesity. Diabetes 2005;54:3190–3197
34. Jocken JW, Langin D, Smit E, et al. Adipose triglyceride lipase and hormone-sensitive lipase protein expression is decreased in the obese insulin-resistant state. J Clin Endocrinol Metab 2007;92:2292–2299
35. Lu M, Sarruf DA, Talukdar S, et al. Brain PPAR-γ promotes obesity and is required for the insulin-sensitizing effect of thiazolidinediones. Nat Med 2011;17:618–622
36. Ryan KK, Li B, Grayson BE, Matter EK, Woods SC, Seeley RJ. A role for central nervous system PPAR-γ in the regulation of energy balance. Nat Med 2011;17:623–626
37. Carlsson LM, Jacobson P, Walley A, et al. ALK7 expression is specific for adipose tissue, reduced in obesity and correlates to factors implicated in metabolic disease. Biochem Biophys Res Commun 2009;382:309–314
38. Arner P, Bernard S, Salehpour M, et al. Dynamics of human adipose lipid turnover in health and metabolic disease. Nature 2011;478:110–113
39. Hotamisligil GS. Inflammation and metabolic disorders. Nature 2006;444:860–867
40. Tilg H, Moschen AR. Adipocytokines: mediators linking adipose tissue, inflammation and immunity. Nat Rev Immunol 2006;6:772–783
41. Lin FT, MacDougald OA, Diehl AM, Lane MD. A 30-kDa alternative translation product of the CCAAT/enhancer binding protein alpha message: transcriptional activator lacking antimitotic activity. Proc Natl Acad Sci USA 1993;90:9606–9610